DOI:10.1021/jf101258x

JOURNAL OF AGRICULTURAL AND FOOD CHEMISTRY
ARTICLE

Chemical Structure and Heterogeneity Differences of Two Lignins from Loblolly Pine As Investigated by Advanced Solid-State NMR Spectroscopy

Kevin M. Holtman,[§] Na Chen,[†] Mark A. Chappell,[#] John F. Kadla,[⊥] Ling Xu,[⊗] and Jingdong Mao*,[†]

[†]Department of Chemistry and Biochemistry, Old Dominion University, 4541 Hampton Boulevard, Norfolk, Virginia 23529, [§]Western Regional Research Center, Agricultural Research Service, U.S. Department of Agriculture, Albany, California 94710, [#]Environmental Laboratory, U.S. Army Corps of Engineers, 3909 Halls Ferry Road, Vicksburg, Mississippi 39180, [⊥]University of British Columbia, 4034-2424 Main Mall, Vancouver, BC V6T 1Z4, Canada, and [⊗]Department of Mathematics and Statistics, James Madison University, Harrisonburg, Virginia 22807

Advanced solid-state NMR was employed to investigate differences in chemical structure and heterogeneity between milled wood lignin (MWL) and residual enzyme lignin (REL). Wiley and conventional milled woods were also studied. The advanced NMR techniques included ^{13}C quantitative direct polarization, various spectral-editing techniques, and two-dimensional $^{1}H-^{13}C$ heteronuclear correlation NMR with ^{1}H spin diffusion. The ^{13}C chemical shift regions between 110 and 160 ppm of two lignins were quite similar to those of two milled woods. REL contained much more residual carbohydrates than MWL, showing that MWL extraction more successfully separated lignin from cellulose and hemicelluloses than REL extraction; REL was also of higher COO, aromatic C−C, and condensed aromatics but of lower aromatic C−H. At a spin diffusion time of 0.55 ms, the magnetization was equilibrated through the whole structure of MWL lignin, but not through that of REL, indicating that REL is more heterogeneous than MWL.

KEYWORDS: Milled wood lignin; solid-state NMR; heterogeneity; spin diffusion; spectral editing

INTRODUCTION

Lignins are reticulated, cross-linked macromolecules composed of phenylpropanoid units (*1*−*4*). The three precursor alcohols of lignins are *p*-coumaryl, coniferyl, and sinapyl alcohols (*5*), producing *p*-hydroxyphenyl (H), guaiacyl (G), and syringyl (S) phenylpropanoid units, respectively. The molecular characterization of lignins is difficult because lignins are complex macromolecules that covalently link to polysaccharides in the plant cell wall and are only partially soluble in a wide range of solvents. Usually, the first step to characterizing lignins is the extraction of representative lignin materials from plant materials such as woods or the production of artificial lignins such as dehydrogenation polymer (DHP) lignins. However, there is concern that extraction can cause structural modifications of lignins or that the isolatable portions are not structurally representative of the whole lignins but biased toward an extractable region of these polymers. Among different isolation procedures for wood lignins, the extraction of milled wood lignin (MWL) is one of the most common ones because it is believed that this method minimizes artifact formation and thus has been considered to be most representative of native lignins from wood.

MWL is isolated typically by ball milling, followed by extraction with aqueous dioxane, which results in a low molecular weight, isolatable fraction of the lignin (*6*−*11*). Chang et al. (*12*) showed that the yield of lignin can be increased by enzymatic degradation of cellulose and then by subsequent solvent extraction (*12*). It has been shown that these fractions are chemically similar (*13*). The residue from this isolation is dubbed residual enzyme lignin (REL) and, due to its insolubility, REL has not been as closely analyzed as MWL (*14*, *15*). Ikeda et al. (*16*), through chemical degradation techniques such as derivatization followed by reductive cleavage, nitrobenzene, and permanganate oxidation, showed that there was a difference in the β-aryl ether content and a higher incidence of condensed C═C linkages (*16*). The question remains whether or not the REL is structurally similar to MWL and whether it has undergone modifications from the rigorous isolation.

Recently, we developed a series of advanced solid-state NMR techniques, especially new spectral-editing techniques, for characterizing complex organic matter in soil, sediment, water, and plant materials (*17*−*20*). Using these systematic techniques, we investigated differences between lignins in unprocessed wood, milled wood, mutant wood, and extracted MWL lignin (*17*). In the present study we applied these advanced solid-state NMR techniques to two lignin samples, MWL and REL, to investigate their structural differences. Also, we included two milled wood samples for comparison to examine whether REL and MWL are representative of lignins in the original woods.

*Author to whom correspondence should be addressed [e-mail jmao@odu.edu; phone (757) 683-6874; fax (757) 683-4628].

 Published on Web 08/20/2010

MATERIALS AND METHODS

Materials. All samples were produced from loblolly pine (*Pinus taeda*). The loblolly pine was a mature tree taken from the Schenck Memorial Forest in Wake County, North Carolina. The wood sample was taken from the sapwood. Sapwood was ground to pass a 20-mesh screen in a Wiley mill and Soxhlet-extracted with 1:2 (v/v) ethanol/benzene for 24 h, followed by ethanol for 24 h, which is referred to as Wiley milled wood (*17*). The Wiley milled wood (100 g) was subject to 1 week of rotary ball-milling with glass balls, followed by 48 h of vibratory ball-milling with steel balls in toluene in 10 g batches, which is called conventional milled wood (*17*). To extract MWL, the Wiley milled wood (100 g) was subjected to 6 weeks of rotary ball-milling with porcelain balls. Twenty-five grams of the milled wood flour was weighed into a 500 mL centrifuge bottle; 250 mL of 1,4-dioxane/water (96:4, v/v) solution was added, and the solution was stirred at room temperature for 24 h under a N_2 atmosphere. The solution was centrifuged, and the supernatant was collected. The remaining solid material was once again dispersed in the 96% (w/w) dioxane solution and the above procedure repeated. The final solid material was washed twice with deionized water and freeze-dried. The solvent from the supernatant was evaporated under reduced pressure to a volume of 100 mL. The concentrated dioxane solution was then added dropwise to deionized water in a freeze-drying flask with stirring to induce precipitation. After freeze-drying, the crude MWL was dissolved in 20 mL of 90% acetic acid (9:1, v/v) and precipitated into deionized water (400 mL). The precipitated lignin was filtered, dissolved in 10 mL of 1,2-dichloroethane/ethanol (2:1, v/v), precipitated into 200 mL of ether, and washed with petroleum ether. The purified MWL was air-dried, ground to further facilitate evaporation of ether, placed in a vacuum oven at 40 °C and 30 in. of Hg overnight, and finally stored in a desiccator under vacuum over P_2O_5 until analysis. The lignin content of the loblolly pine is 27.3%. After isolation, the total yield of milled wood lignin (MWL) was 18.1% on a lignin basis. The MWL has a lignin content of 87.7%.

Cellulolytic enzyme lignin (CEL) was extracted from the insoluble residue after the dioxane extraction by standard methods for MWL isolation (*12*). We recently showed that CEL is similar to MWL and hence it is not analyzed here (*13*). The insoluble residue from 96% dioxane extraction of CEL is the REL and represents the remaining lignin present in the original whole wood material.

NMR Spectroscopy. All of the experiments, except the quantitative direct polarization/magic angle spinning (DP/MAS) and DP/MAS with recoupled dipolar dephasing, were performed on a Bruker DSX spectrometer at 100 MHz for ^{13}C, using MAS in a 7 mm double-resonance probehead. DP/MAS and DP/MAS with recoupled dipolar dephasing experiments were conducted using a 4 mm double-resonance probe at 14 kHz.

^{13}C DP/MAS and DP/MAS with Recoupled Dipolar Dephasing. NMR experiments were performed at a spinning speed of 14 kHz. The 90° ^{13}C pulse length was 4 μs. Recycle delays were 200 s, determined by the cross-polarization/spin−lattice relaxation time/total sideband suppression (CP/T_1-TOSS) technique to ensure that all carbon sites were >95% relaxed (*21*). To obtain quantitative information on the nonprotonated carbon fraction, DP/MAS ^{13}C NMR with recoupled dipolar dephasing was used (*22*). The dipolar dephasing time was 68 μs.

^{13}C CP/TOSS and ^{13}C CP/TOSS with Dipolar Dephasing. Qualitative composition information was obtained with good sensitivity by ^{13}C cross-polarization/total sideband suppression (CP/TOSS) NMR experiments at a spinning speed of 5 kHz and a cross-polarization (CP) time of 1 ms, with a ^1H 90° pulse length of 4 μs and a recycle delay of 1 s. We checked the shapes of 1 s spectra and found that they are the same as those of the fully relaxed 3 s spectra. Four-pulse total suppression of sidebands (TOSS) (*23*) was employed before detection, and two-pulse phase-modulated (TPPM) decoupling was applied for optimum resolution. The corresponding subspectrum with signals of nonprotonated carbons and mobile groups such as rotating CH_3 was obtained by ^{13}C CP/TOSS combined with 40 μs dipolar dephasing.

^{13}C Chemical Shift Anisotropy Filter (CSA). To separate the signals of anomeric carbons (O—C—O) from those of aromatic carbons, both of which may resonate between 90 and 120 ppm, the aromatic carbon signals were selectively suppressed by a five-pulse ^{13}C chemical shift anisotropy (CSA) filter with a CSA filter time of 35 μs (*22*, *24*). To select the signals of nonprotonated O—C—O (ketal) carbons, which may extend to 120 ppm, this CSA filter was combined with a dipolar dephasing time of 40 μs. In a complementary experiment, selective spectra of protonated anomerics (O—CH—O, acetals) were obtained by CSA filtering after a 50 μs short CP. The recycle delay was 1 s. The details of this robust and efficient technique have been described elsewhere (*24*).

CH Spectral Editing. For CH (methine) selection, a robust method based on C—H multiple-quantum coherence (*25*) was used at 4 kHz MAS. CH-group multiple-quantum coherence is not dephased by the spin-pair CH dipolar coupling, whereas CH_2 group coherence is dephased by dipolar coupling of the carbons to the two protons. The first of a pair of recorded spectra contains signals of CH as well as residual quaternary-carbon and CH_3 peaks that are removed by taking the difference with a second spectrum acquired with the same pulse sequence except for an additional 40 μs dipolar dephasing before detection.

$^1H-^{13}C$ Heteronuclear Correlation (HETCOR) NMR with Spin Diffusion. The domains and heterogeneities of lignins can be investigated using 2D HETCOR with ^1H spin diffusion (*17*−*20*, *26*). These experiments were performed at a spinning speed of 6.5 kHz using Hartmann−Hahn cross-polarization with ^1H spin diffusion. The CP time was 1 ms, with an effective spin diffusion time of 0.25 ms. The t_1 dimension was incremented in 96 steps of 5 μs. The effective mixing times inserted were 0.25, 0.55, and 1.25 ms for MWL and 0.25, 0.55, and 5.25 ms for REL, respectively. ^1H slices at the ^{13}C chemical shifts of 130 ppm for aromatics and 72 ppm for OCH were extracted to observe whether the magnetization was equilibrated or not between aromatic and carbohydrate protons at different spin diffusion times.

RESULTS AND DISCUSSION

Representativeness of Lignins. Figure 1, panels **a**−**d** and panels **e**−**h**, shows the assignments of Wiley-milled wood and conventional milled wood, respectively, with the assistance of spectral-editing techniques. Generally, compared with the spectra of Wiley-milled wood, those of conventional milled wood are broad, illustrating that milling renders crystalline structures in the wood amorphous due to the intensive energy input. **Figure 1**, panels **a** and **e**, are full ^{13}C CP/TOSS spectra used for reference. They show relatively sharp peaks in the aliphatic region between 20 and 110 ppm and relatively broad ones for sp^2-hybridized carbons between 110 and 220 ppm. The selection of sp^3-hybridized alkyl carbons is achieved by using a CSA filter (**Figure 1b**,**f**), which clearly resolves C1 of carbohydrate rings. **Figure 1**, panels **c** and **g**, display dipolar-dephased spectra showing nonprotonated carbons and mobile segments such as CH_3 and OCH_3. The dipolar-dephased spectra clearly select well-resolved signals of CH_3 of CH_3—COO, OCH_3, nonprotonated aromatics, aromatic C—O, and COO of CH_3—COO groups. Small residual OC peaks are also observed, which may be due to either nonprotonated OC or protonated, mobile OCH and OCH_2 groups. The CH selection technique shows signals of aromatic CH, OCHO, and CHOH (**Figure 1d**,**h**). The three major constituents of wood are cellulose, hemicelluloses, and lignin. On the basis of detailed spectral-editing spectra and the literature (*27*), the assignments of the major components of the cell wall in loblolly pine in the ^{13}C CP/TOSS spectra of Wiley-milled wood can be made. The wood ^{13}C spectra are assigned as follows: 21.6 ppm, CH_3 of CH_3COO of hemicellulose; 56 ppm, OCH_3 of $ArOCH_3$ of lignin; 64−60 ppm, C_γ—OH of lignin; 63 ppm, CH_2OH of carbohydrates (amorphous C_6 of cellulose); 66 ppm, CH_2OH of carbohydrates (crystalline C_6 of cellulose); 72 ppm, CHOH of carbohydrates (C_2, C_3, and C_5 of cellulose); 76−72 ppm, C_α—OR of lignin; 75 ppm, CHOH of carbohydrates (C_2, C_3, and C_5 of cellulose); 86−82 ppm, C_β—OR of lignin; 84 ppm, CHOH of carbohydrates (amorphous C_4 of cellulose); 89 ppm, CHOH of carbohydrates (crystalline C_4 of cellulose); 105 ppm, OCHO of carbohydrates (C_1 of cellulose); 112 ppm, aromatic CH (G_2 of lignin), 115 ppm, aromatic CH (G_5 of lignin); 120 ppm, aromatic CH (G_6 of lignin);

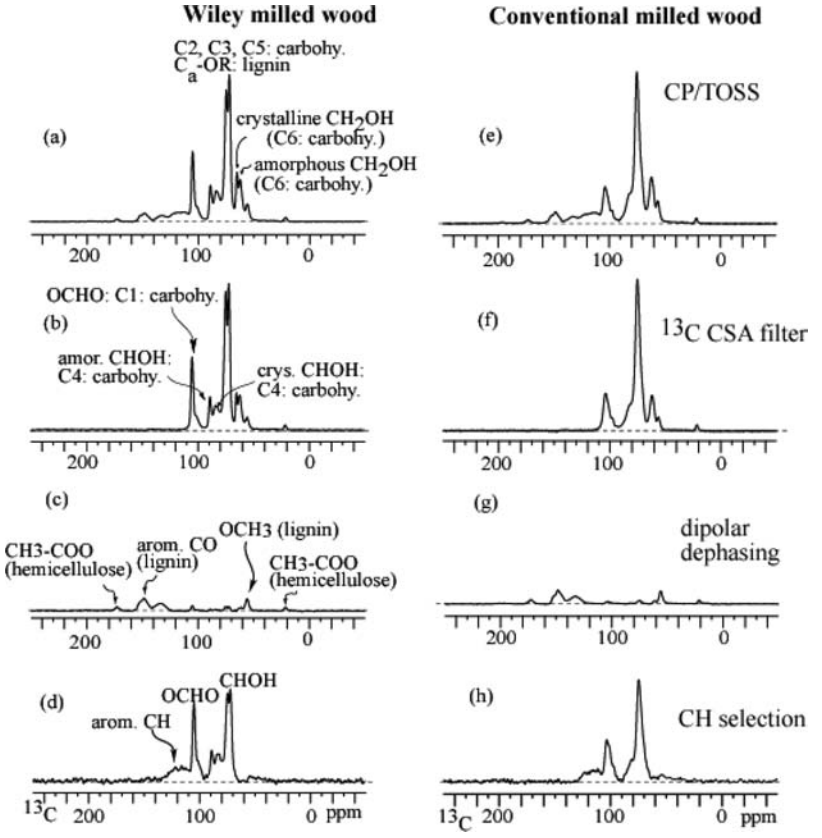

Figure 1. Spectral-editing spectra of (left) Wiley-milled wood and (right) conventional milled wood: (**a**, **e**) full CP/TOSS spectra for reference; (**b**, **f**) selection of alkyl carbons with a CSA filter; (**c**, **g**) dipolar dephasing spectra showing unprotonated carbons and mobile segments such as CH_3 and OCH_3; (**d**, **h**) CH-only spectra.

Table 1. NMR Chemical Shifts of Wood

moiety	chemical shift (ppm)
aldehyde/ketone (C═O)	220−187
−COO/CH_3COO	173
aromatic C—O ($G_{3(e)}$ and $G_{3(ne)}$)	153−147
aromatic C—O ($G_{4(e)}$ and $G_{4(ne)}$)	147−143
aromatic C—C ($G_{1(e)}$)	137−134
aromatic C—C ($G_{1(ne)}$)	131
aromatic C—H (G_6 of lignin)	120
aromatic CH (G_5 of lignin)	115
aromatic CH (G_2 of lignin)	112
OCHO of carbohydrates (C_1 of cellulose)	105
CHOH of carbohydrates (crystalline C_4 of cellulose)	89
CHOH of carbohydrates (amorphous C_4 of cellulose)	84
C_β-OR of lignin	86−82
CHOH of carbohydrates (C_2, C_3, C_5 of cellulose)	75
C_α-OR of lignin	76−72
CHOH of carbohydrates (C_2, C_3, C_5 of cellulose)	72
CH_2OH of carbohydrates (crystalline C_6 of cellulose)	66
CH_2OH of carbohydrates (amorphous C_6 of cellulose)	63
C_γ—OR of lignin	64−60
OCH_3 of lignin	56
CH_3 of hemicelluloses	21.6

131 ppm, nonprotonated aromatics $G_{1(ne)}$; 137−134 ppm, nonprotonated aromatics $G_{1(e)}$; 147−143 ppm, nonprotonated aromatics ($G_{4(e)}$ and $G_{4(ne)}$); 153−147 ppm, nonprotonated aromatics ($G_{3(e)}$ and $G_{3(ne)}$); and 173 ppm (COOR, CH_3COO) (*27*). Note that the subscript "e" refers to "etherified" and "ne" to "non-etherified" (*27*). Because softwoods such as loblolly pine contain primarily guaiacyl lignin, we do not include the assignments of S and H lignins here. The detailed assignments are shown in **Table 1**. There should be small signals around 200 ppm attributed to ketones and aldehydes (*17*), but the current vertical scaling of the spectra made them almost invisible. The spectra of conventional milled wood are broad due to loss of crystallinity caused by milling. The resolved peak signals at 66 and 89 ppm of crystalline cellulose in Wiley milled wood have eroded to a broader amorphous signal centered at 63 and 84 ppm in conventional milled wood, overlapping even more extensively with the likewise broad lignin chemical shifts.

Figure 2, panels **a**−**d**, compares the extracted lignins with those in two wood samples to reveal whether lignin extractions representatively isolate lignins from the whole woods. To facilitate the comparison, we vertically scale up the ^{13}C CP/TOSS spectra of Wiley-milled wood (**Figure 2a**) and conventional milled wood (**Figure 2b**) so that their sp^2-hybridized carbon signals above 110 ppm, which are mostly assigned to lignin signals, can match those of MWL lignin (**Figure 2c**) and REL (**Figure 2d**). Obviously, the regions between 110 and 160 ppm of two lignins are quite similar to those of Wiley-milled wood and conventional milled wood. For the two lignins, the MWL spectrum (**Figure 2c**) shows the isolated lignin signals with small contributions (<5%) from carbohydrates; in contrast, that of REL (**Figure 2d**) reveals significant signals of cellulose or hemicellulose from the region between 65 and 95 ppm and CH_3—COO of hemicellulose at 21.6 and 173 ppm, in addition to lignin components similar to MWL. The detailed differences of the two lignins will be described below.

Spectral Editing for Specific Functional Groups of Lignins. **Figure 3** shows a series of ^{13}C CP/MAS NMR spectra for the two lignins acquired with suitably designed radiofrequency pulse sequences to select subspectra of specific types of chemical functional groups, such as dipolar dephasing, ^{13}C chemical shift

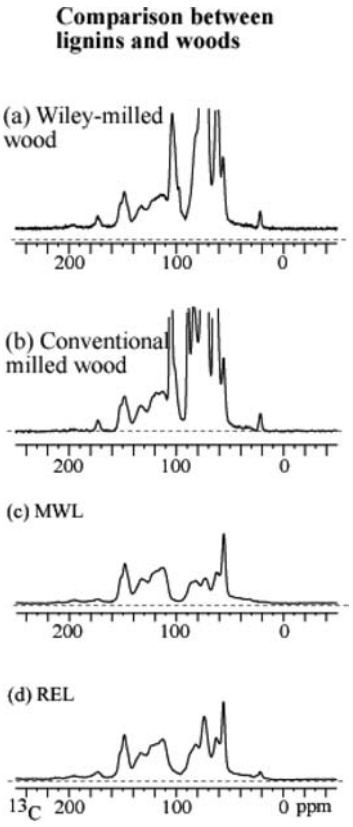

Figure 2. Comparison of ^{13}C CP/TOSS spectra of milled woods and lignins to show how lignin extraction works; ^{13}C CP/TOSS of (**a**) vertically scaled Wiley-milled wood, (**b**) vertically scaled conventional milled wood, (**c**) MWL, and (**d**) REL.

anisotropy filter (*22*, *24*), and CH selection (*25*). Panels **a** and **g** of **Figure 3** are ^{13}C CP/TOSS spectra of MWL and REL, respectively. These spectra show the entire spectrum without spinning-sideband interference, provide qualitative structural information, and are used primarily as reference spectra for spectral editing.

The corresponding CP/TOSS spectra after 40 μs of dipolar dephasing (**Figure 3b**,**h**) exhibit solely signals of nonprotonated carbons and carbons of mobile groups, including rotating CCH_3 and OCH_3 groups, which have a decreased C−H dipolar coupling due to their fast motions. For REL, we observe CH_3 of CH_3COO at 21.6 ppm, OCH_3 of $ArOCH_3$ at 56 ppm, nonprotonated aromatics around 133 ppm, aromatic C—O at 148 ppm with a shoulder at 153 ppm, COO of CH_3COO at 173 ppm, and C=O ketones around 196 ppm. The nonprotonated aromatics around 133 ppm can be primarily assigned to G1(e). The aromatic C—O at 148 ppm is dominantly attributed to G1 and G4, but only slightly to S3(ne) and S5(ne) because this is a guaiacyl-based lignin. This guaiacyl-dominant lignin can also be confirmed by the dominant 148 ppm but only a small shoulder for 153 ppm, which is assigned to S3(e) and S5(e). The combination of the peaks at 21.6 and 173 ppm indicates that this lignin also contains significant hemicellulose. The dipolar-dephased spectrum of MWL is similar to that of REL, except that the peaks of hemicelluloses at 21.6 and 173 ppm are barely above the baseline (**Figure 3b**). This indicates that the MWL extraction method is more successful in separating lignin from cellulose and hemicellulose than the REL extraction procedure.

The CP/TOSS spectra after a ^{13}C CSA filter of 35 μs, which exhibit only sp^3-hybridized-carbon signals, are displayed in **Figure 3c**,**i**. In particular, this technique separates overlapping anomerics (O—C—O) from aromatics between 90 and 120 ppm. A clear O—C—O band is displayed in this region for REL, indicating significant residual carbohydrates (**Figure 3i**), whereas the anomeric carbon is practically absent from the MWL spectrum as expected. The combination of this filter technique with short CP selects subspectra of only protonated sp^3-hybridized-carbon sites (**Figure 3d**,**j**). The combination of this filter technique with dipolar dephasing leads to subspectra of solely nonprotonated or mobile sp^3-hybridized carbon sites (**Figure 3e**,**k**). For REL, only a very slight signal of quaternary O—C_q—O around 105 ppm is present in **Figure 3k**; in contrast, predominant OCO belong to OCHO, as demonstrated in **Figure 3j** and by comparison of **Figure 3j**,**i**. Obviously, aliphatic OCO groups are dominantly protonated in this lignin. For MWL, we observe only a slight protonated anomeric signal above baseline in **Figure 3d** but almost no nonprotonated anomeric signal around 100 ppm in **Figure 3e**. This finding confirms that there are significant carbohydrate residues in REL, but only small amounts in MWL. This can also be confirmed by the differences in the region between 65 and 95 ppm of their ^{13}C CP/TOSS spectra (**Figure 3a**,**g**). A sharp CHOH peak belonging to C_2, C_3, and C_5 of cellulose is observed in **Figure 3g**, not in **Figure 3a**.

The CH-only spectra of MWL and REL indicate that they consist of a broad range of CH signals between 55 and 30 ppm, OCH around 60−90 ppm, and aromatic CH and anomeric OCHO around 100−130 ppm (**Figure 3f**,**l**). The aliphatic CCH arises primarily from the condensed lignin side-chain substructures. The aliphatic CCH could be from the structures of spirodienone, pinoresinol, and secoisolariciresinol (*17*). The OCH signals around 60−90 ppm are from C_4 and $C_{2,3,5}$ of carbohydrates and C_α—OR, C_β—OR, and also C_γ—OH of lignin. The CH band around 100−130 ppm can be attributed to C1 of carbohydrates (106 ppm) and $G_{2,5,6}$ of lignins.

Heterogeneities of Lignin Based on 2D HETCOR with ^{1}H Spin Diffusion. 2D HETCOR with ^{1}H spin diffusion can provide the heterogeneities and domains of organic materials such as lignins (*17*, *26*). REL contains more hemicelluloses and cellulose than MWL. Using spin diffusion, we can explore the heterogeneities between REL and MWL, that is, how lignin components are associated with other components such as residual carbohydrates. For complex natural organic matter without obvious separate rigid and mobile components, various spin diffusion times inserted into 2D HETCOR have proven to be an ideal approach for investigating domains and heterogeneities. We have used this approach to investigate the heterogeneities of humic acids (*17*−*20*). Here, instead of using Lee−Goldburg CP (LGCP) as before, we use Hartmann−Hahn CP (HHCP). During HHCP, the effective spin diffusion time is one-fourth of the CP time. To observe how long it will take to reach magnetization equilibration throughout the whole lignin structure, we extract carbon slices at two different positions of protons, that is, one near carbohydrate OCH around 4.1 ppm and another near aromatic protons around 7 ppm, from 2D HETCOR spectra at different spin diffusion times. The judgment is that if the two carbon slices are virtually identical, then magnetization is equilibrated throughout the whole lignin structure.

Figure 4 is the 2D HETCOR with spin diffusion of MWL. The spin diffusion times for **Figure 4a**,**b**,**c** are 0.25, 0.55, and 1.25 ms, respectively. Their corresponding extracted carbon slices are stacked and shown in **Figure 4d**,**e**,**f**, respectively. At a spin diffusion time of 0.25 ms, the carbon slice extracted at the carbohydrate OCH protons (thick line) still does not match the slice extracted at aromatic protons (thin line). Their sp^2-hybridized carbon portions are almost the same, but large differences still exist for their sp^3-hybridized carbons. This suggests that dominant MWL and the small amounts of residual carbohydrates

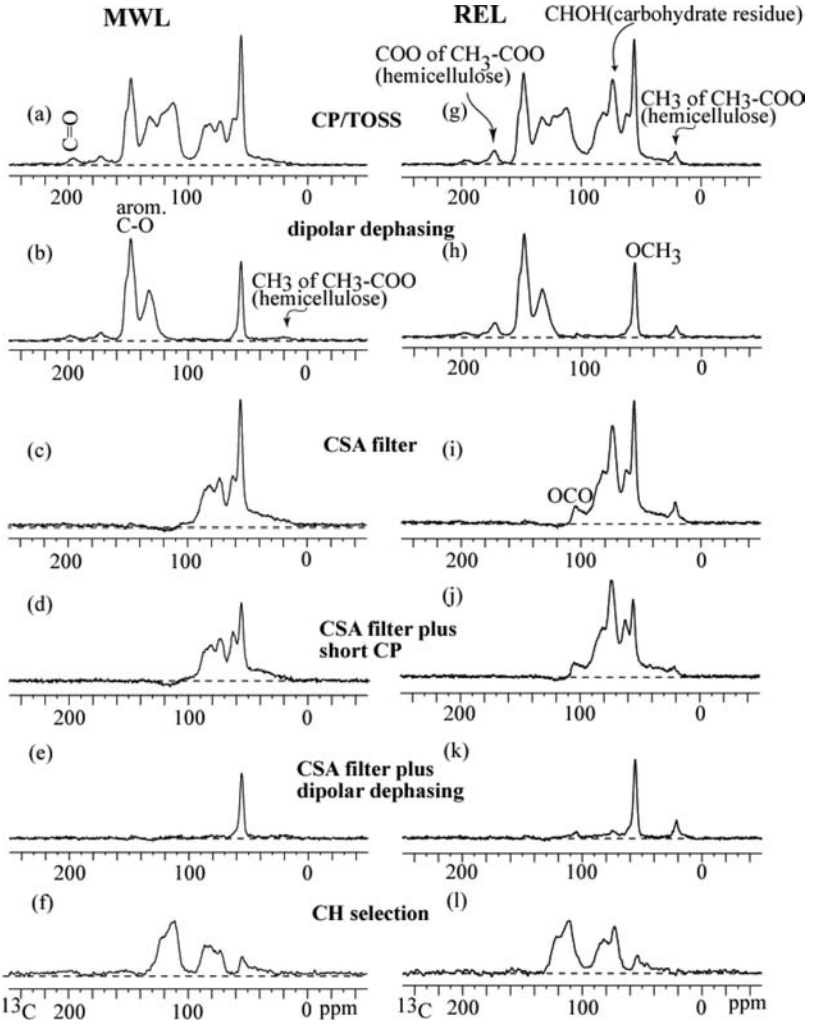

Figure 3. Spectral editing for MWL (**a**−**f**) and REL (**g**−**l**): (**a**, **g**) full CP/TOSS spectra for reference with a contact time of 1 ms; (**b**, **h**) dipolar dephasing spectra showing unprotonated carbons and mobile segments such as CH_3 and OCH_3 with 40 μs dephasing time; (**c**, **i**) selection of alkyl carbons with a CSA filter, which in particular identifies OCO carbons typical of sugar rings (CSA filter time = 35 μs); (**d**, **j**) selection of protonated alkyl carbons with a CSA filter and short CP, in particular OCHO around 100 ppm (CSA filter time = 35 μs; CP time = 50 μs); (**e**, **k**) selection of nonprotonated and mobile alkyl carbons with a CSA filter and dipolar dephasing, which in particular identifies OC(RR′)O carbons (CSA filter time = 35 μs; dipolar dephasing time = 40 μs); (**f**, **l**) selection of CH groups.

detected by spectral-editing techniques in MWL are heterogeneous. At a spin diffusion of 0.55 ms, the two carbon slices are matched and virtually identical, indicating that all of the magnetization is equilibrated throughout the whole MWL; the same result is shown for a spin diffusion time of 1.25 ms.

Figure 5 is the 2D HETCOR with spin diffusion of REL. The spin diffusion times for **Figure 5a**,**b**,**c** are 0.25, 0.55, and 5.25 ms, respectively. Their corresponding extracted carbon slices are stacked and shown in **Figure 5d**,**e**,**f**, respectively. At a spin diffusion time of 0.25 ms, the carbon slice extracted at the carbohydrate OCH protons (thick line) does not match the slice extracted at aromatic protons (thin line). Both their sp^2- and sp^3-hybridized carbon portions cannot be matched. At a spin diffusion of 0.55 ms, their sp^2-hybridized carbon portions are almost the same, but certain differences still exist for their sp^3-hybridized carbon parts, especially for the OCH signal of carbohydrates at ~72 ppm, in contrast to MWL. This indicates that REL is more heterogeneous than MWL. At a spin diffusion of 5.25 ms, the two carbon slices are matched and virtually identical, indicating that all of the magnetization is finally equilibrated throughout the whole REL.

Synopsis of Assignments of Lignins and Their Carbohydrate Residues Based on Advanced Spectral-Editing NMR. The three lignin units are *p*-hydroxyphenyl (H), guaiacyl (G), and syringyl (S) phenylpropanoids. Lignins from loblolly pine are primarily G lignins. Thus, we mainly focus on the assignment of G lignin. On the basis of Matinez et al. (*27*), the specific chemical shifts of the carbon in lignin can be assigned as follows: 153 ppm, C_3 and C_5 in S units (e), which is small in the lignins of the present study; 148 ppm, C_3 and C_4 in G units; 136 ppm, C_1 in G units (e); 120 ppm, C_6 in G units; 115 ppm, C_5 in G units; 112 ppm, C2 in G units; 86−82 ppm, C_β in β-*O*-4-linked side chains; 76−72 ppm, C_α—OH in β-*O*-4-linked side chains; 64−60 ppm, C_γ—OH; 56 ppm, OCH_3 on the aromatic ring; 52−15 ppm, aliphatic C—C resonances (*27*). Martinez et al. (*27*) also indicated that the most significant differences between the hardwood and softwood lignins were observed at 153 and 105 ppm. The major signals can be observed in the hardwood lignins, but only small shoulders are detected in softwood lignin at the two chemical shifts, 153 and 105 ppm. The spectra in the present study are in agreement with the dominance of G units in softwood lignin (**Figure 3a**,**b**).

Quantitative Structural Information. Quantitative ^{13}C NMR spectra of the two lignin samples, acquired using direct polarization (DP) at 14 kHz MAS, are shown in **Figure 6a**,**c**. The corresponding quantitative subspectra of nonprotonated carbons and

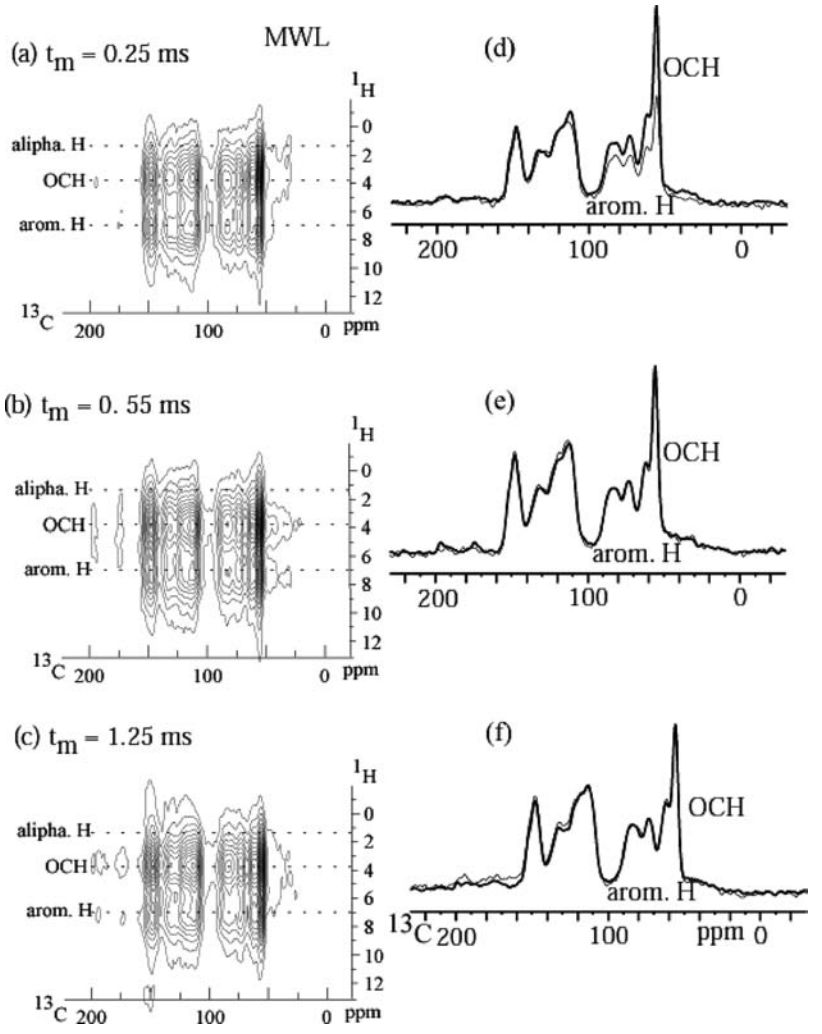

Figure 4. 2D HETCOR with ^{1}H spin diffusion and comparison of aromatic and OCH proton slices for MWL; 2D HETCOR spectra with 1 ms HHCP and (**a**) t_m = 6 μs, (**b**) t_m = 0.3 ms, and (**c**) t_m = 1 ms. Their corresponding aromatic and OCH proton slices are shown in **d**, **e**, and **f**, respectively. Effective t_m times for **a**, **b**, and **c** are 0.25, 0.55, and 1.25 ms, respectively.

carbons of mobile segments (**Figure 6b**,**d**) were obtained by combining DP/MAS with recoupled dipolar dephasing of 68 μs (*22*). Compared with the corresponding ^{13}C CP/TOSS spectra (**Figure 3a**,**g**), the DP/MAS spectra are of enhanced sp^2-hybridized carbons, which is in agreement with our previous results (*21*, *28*).

We integrate the quantitative DP/MAS spectra into nine chemical shift regions: 0−48 ppm, acetyl CH_3 and other aliphatic C not bound to oxygen; 48−61.2 ppm, OCH_3 groups and lignin condensed aliphatic side chain units; 61.2−68 ppm, C_γ—OH and C_6 of residual carbohydrate (CH_2OH); 68−80.7 ppm, C_α—OH in β-*O*-4-linked side chains, and C_2, C_3, and C_5 of residual carbohydrate (CHOH); 80.7−98 ppm, C_β in β-*O*-4-linked side chains and C_4 of residual carbohydrate (CHOH); 98−142 ppm, C_1 in G units (etherified), C_5 in G units, and C_1 of residual carbohydrate; 142−165 ppm, C_3 and C_4 in G units; 165−187 ppm, acetyl COO; and 187−220 ppm, ketones and aldehydes (**Table 2**). The most conspicuous difference is the region between 68 and 98 ppm, where C_{2-5} of residual carbohydrates and C_β and C_α—OH in β-*O*-4-linked side chains are present; REL contains much more residual carbohydrates than MWL. **Table 3** shows the contents of different functional groups of MWL and REL on a carbon per aromatic rings basis, including those of solution NMR for MWL. In **Table 4**, the lignin aliphatic side-chain structures and total carbons as determined by quantitative direct polarization combined with spectral-editing techniques are summarized.

On the basis of **Tables 2**−**4**, we discuss the detailed, quantitative structural differences of the two lignins, primarily ordered from downshift to upshift according to their ^{13}C NMR resonance positions. Because we have solution NMR results for MWL, its experimental results obtained using the advanced solid-state NMR described here will be also compared to those of solution NMR (*29*) for this lignin.

Ketones and Aldehydes. In our previous study, the quantities of structures **I**−**IV** (**Figure 7**) were estimated by integration of the chemical shifts between 220 and 187 ppm (*17*). By normalizing the aromatic region (165−98 ppm) of ^{13}C CP/TOSS spectrum to a value of 6.12 analogous to solution NMR (*30*−*32*), it was determined that structures **I**−**IV** represent 0.25 carbon per aromatic ring (C/Ar) in the MWL (*17*).

Using the identical MWL but quantitative data with ^{13}C DP/MAS, a similar value of 0.23 C/Ar for all carbonyl structures (**I**−**IV**) was obtained. Solution NMR returned a value of 0.14 C/Ar, somewhat lower than that determined by employing solid-state NMR. The carbonyl content of the REL was determined to be 0.24 C/Ar, similar to that of the MWL. Note that solid-state NMR is more reliable in quantification than solution NMR, as discussed in ref *17*.

−*COO Groups*. Carboxyl structures, centered around 187−164 ppm, previously were estimated to be 0.05 C/Ar for the MWL material by solution NMR; however, DP/MAS integration resulted

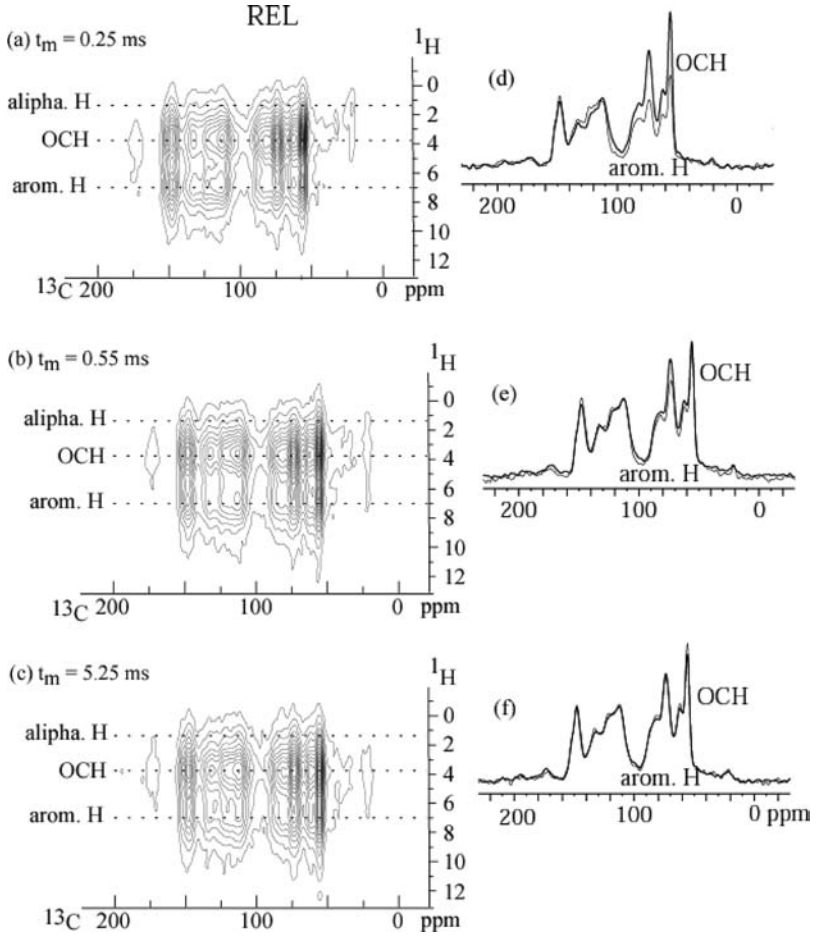

Figure 5. 2D HETCOR with ^{1}H spin diffusion and comparison of aromatic and OCH proton slices for REL; 2D HETCOR spectra with 1 ms HHCP and (**a**) t_m = 6 μs, (**b**) t_m = 0.3 ms, and (**c**) t_m = 5 ms. Their corresponding aromatic and OCH proton slices are shown in **d**, **e**, and **f**, respectively. Effective t_m times for **a**, **b**, and **c** are 0.25, 0.55, and 5.25 ms, respectively.

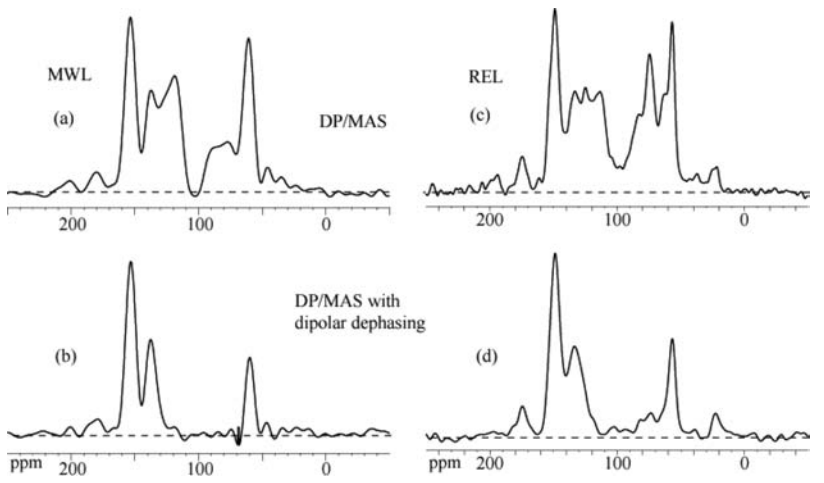

Figure 6. Quantitative structural information obtained with DP/MAS and DP/MAS with recoupled dipolar dephasing: (**a**, **b**) spectra of MWL; (**c**, **d**) spectra of REL; (**a**, **c**) DP/MAS; (**b**, **d**) DP/MAS with recoupled dipolar dephasing.

Table 2. Percentage of Total Spectral Area Assigned to Different Functional Groups Obtained from ^{13}C DP NMR Combined with Spectral-Editing Techniques[a]

ppm	220−187	187−165	165−142	142−98	98−80.7	80.7−68	68−61.2	61.2−48	48−0
MWL	2.1%	3.3%	20.7%	35.9%	4.9%	7.1%	3.4%	16.1%	6.2%
REL	1.9%	3.3%	17.7%	31.3%	8.4%	13.3%	5.9%	11.2%	4.5%

[a] Anomerics OCO of sugars around 105 ppm are corrected on the basis of ^{13}C CSA filter; spinning sidebands are corrected on the basis of a protocol described elsewhere (*22*, *24*). Percentages in the table are representative of the contributions to the spectrum in percent or carbons per 100 carbons.

Table 3. Contents of Different Functional Groups of MWL and REL on a Carbon per Aromatic Ring Basis, Including Those of Solution NMR Data for MWL

	solution (*29*)	solid state		
			C/Ar	
spectral region	MWL (C/Ar)	methodology[a]	MWL	REL
total carbons	N/D	DP	10.77	12.49
−C═O structures	0.14	DP	0.23	0.24
−COO structures	0.05	DP	0.36	0.41
oxygenated aromatic carbons	2.12	DP/DD/CH	2.24	2.21
aromatic carbon−carbon structures	1.54	DP/DD	1.55	1.94
aromatic methine carbons	2.46	DP/diff	2.34	1.97
aliphatic side-chain carbons	2.29	DP/DD	2.92	2.97
carbohydrates	N/D	CSA	0.27	1.60
methoxyl content	0.97	DD	1.12	1.15

[a] Abbreviations: DP, direct polarization/magic angle spinning (DP/MAS); DD, dipolar dephasing; CH, C—H selection; CSA, ^{13}C chemical shift anisotropy filter; diff, calculated by difference. Experimental uncertainties due to noise are ca. 1−2% of the ratios.

in a much higher contribution of 0.36 C/Ar. The REL has a value of 0.41 C/Ar, which could be partially explained by the higher carbohydrate residues with the corresponding methyl resonance at 21.6 ppm. The drastic difference between the results from the solid-state DP and solution NMR experiments accentuates nonquantification of solution NMR.

Aromatic C—O. The aromatic C—O fraction was quantified via the integration of 165−142 ppm chemical shifts in ^{13}C DP/MAS spectra and is composed of the C_3, C_4, and etherified C_5 on the aromatic ring. On the basis of the known lignin biosynthesis pathways and the low expected content of H-lignin in the softwood, it is anticipated that the substitution at C_3 and C_4 with oxygenated components, whether etherified or non-etherified, would be very close to a total of 2 per aromatic ring. The contribution of aromatic C—O was calculated by solution NMR and determined to be 2.12 per aromatic ring for the MWL (*13*), slightly lower than the 2.24 moieties per aromatic ring as determined by ^{13}C DP/MAS. This is higher than has been previously determined by ^{13}C CP/TOSS (1.92/aromatic ring), suggesting that both CP and solution NMR could fail to detect some aromatic C—O. Nevertheless, they are both close to 2. Integration of the REL reveals a very similar 2.21 units per aromatic ring.

Nonprotonated Aromatic C—C. Nonprotonated aromatic C—C linkages, namely, the C_1 and those subunits containing condensed linkages through the C_5 position including the biphenyl (5−5′, **V**, **Figure 7**) and the phenylcoumaran (*β*-5′, **VI**), are represented by chemical shifts centered from 142 to 125 ppm. The nonprotonated aromatic C—C groups can be calculated on the basis of the spectra of ^{13}C DP/MAS with recoupled dipolar dephasing (*22*), returning a value of 1.55 C/Ar for MWL, corroborated by solution NMR, which resulted in 1.55 C/Ar (*29*). The REL, on the other hand, contains a higher aromatic C—C with 1.94 per aromatic ring, supporting the assertion that the REL contains a higher degree of middle lamella lignin than the MWL, which is derived predominately from the secondary wall (*16*).

Protonated Aromatic C—H. The percentage of protonated aromatic carbons was obtained by difference from the quantitative ^{13}C DP/MAS spectra and DP/MAS with recoupled dipolar dephasing by integrating the region of 142−98 ppm and adding spinning sideband intensity, on the basis of the method described in ref *22*. Also, the overlapped anomerics around 105 ppm are identified by ^{13}C CSA filter and subtracted from the integration. The contribution of aromatic C—H for the MWL is 2.34 C/Ar, which is lower than that previously determined by solution NMR (2.46 C/Ar). As can be seen in **Table 3**, the aromatic C—C is increased by 0.12 C/Ar, which is exactly the difference in the integration of the aromatic C−H. The difference could potentially be explained by limitations of integration in the solution NMR experiment, which did not employ spectral-editing techniques to separate and quantify specific functional groups. For instance, the DP/MAS spectrum with dipolar dephasing (**Figure 6b**,**d**) clearly shows nonprotonated C—C around 120 ppm that would be included in the aromatic C—H for a traditional integration in solution NMR. The solid-state determination of aromatic C—C is performed from integration of the dipolar dephasing spectrum and therefore accounts for these structures properly. An example of a possible structure responsible for this chemical shift would be the C_1 ($\delta_C \sim 123$ ppm) in benzoic acid (**XV**) type structures and would partially corroborate the high content of −COO structure (**Figure 7**).

Table 4. Summary of the Aliphatic Lignin Side Chain Structures and Total Carbons As Determined by Quantitative Direct Polarization Combined with Spectral-Editing Techniques

			C/Ar	
spectral region	chemical shift range (ppm)	methodology[a]	MWL	REL
total aliphatic side-chain carbons	98−0	DP/DD	2.95	2.97
O—CH−	98−68	CH	1.31	0.92
O—CH_2−	68−57	diff	0.66	1.15
β-*O*-4′ structures		DP/CH	0.64	0.78
methoxyl content	57−54	DD	1.12	1.15
total aliphatic C—C	61−0	DP	0.84	0.88
−CH—C	61−48	CH	0.34	0.32
−CH—C	48−30	CH	0.23	0.26
−CH_2—C	48−30	diff	0.15	0.02
−CH_3	30−0	DD	0.28	0.28

[a] Abbreviations: DP, direct polarization/magic angle spinning (DP/MAS); DD, dipolar dephasing; CH, C—H selection; CSA, ^{13}C chemical shift anisotropy filter; diff, calculated by difference.

The REL has a C/Ar of only 1.97 for the aromatic C—H, indicating that it is highly substituted on the aromatic ring and thus is much lower than the MWL. Its DP/MAS with recoupled dipolar dephasing (**Figure 6d**) shows significant overlap for signals of nonprotonated aromatics and aromatic C—O groups. This overlap is much less significant in the MWL (**Figure 6b**). This indicates that the aromatics of REL are structurally different from those of MWL, consistent with their differences in substitutions. Aliphatic C═C structures that could potentially resonate around this chemical shift region are coniferyl alcohol, coniferaldehyde, or *p*-coumaric acid. Additionally, the CH selection spectrum of both preparations shows tailings past 130 ppm, indicating the possibility that these structures are present. The data presented here show the advantages of spectral-editing techniques for identifying and quantifying specific functional groups.

Degree of Aromatic Condensation. As discussed previously, on the basis of DP/MAS we can obtain the percentage of aromatic C—O groups, and using DP/MAS with recoupled dipolar dephasing, we can obtain the percentage of aromatic C—C. This allows for more accurate calculation of the ratio of the aromatic C—O to the aromatic C—C, that is, the degree of aromatic condensation (*14*,*32*). In the past, determining the degree of aromatic condensation was tenuous and also could be inaccurate because it is difficult to obtain a precise integration without deconvolution. However, deconvolution for heavily overlapped bands such as those of lignins is not reliable. In contrast, our protocol is more straightforward as it does not rely on deconvolution of overlapping peaks. Also, we resort to quantitative DP/MAS. It is estimated that the aromatic condensations of MWL and REL are 0.27 and 0.46, respectively.

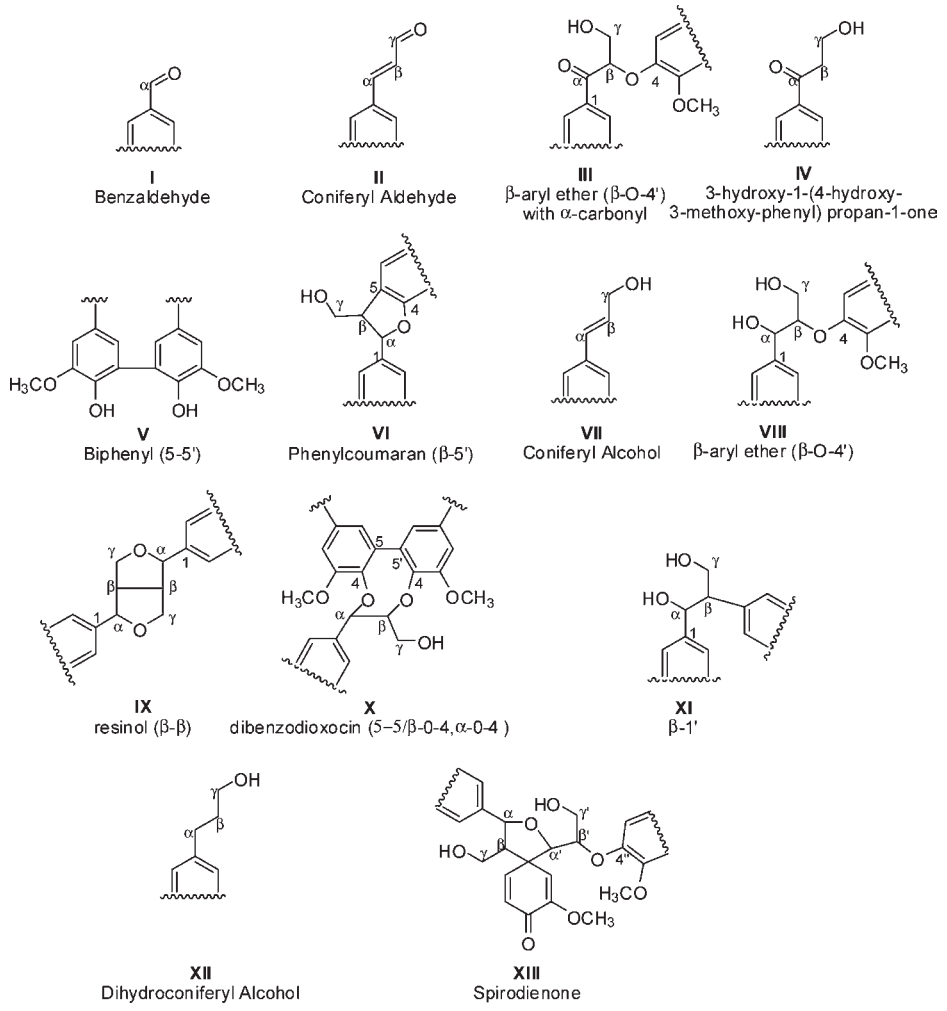

Figure 7. Commonly found interunit linkages in lignin preparations.

Estimation of β-O-4′ Substructures. On the basis of the known structures in MWL, the chemical shift region from 98 to 80 ppm is predominately attributed to C_α from *β*-5′, *β*-*β*′, and *β*-1′ moieties and C_α and C_β from *β*-*O*-4′ structures, including dibenzodioxocin (**X**) (**Figure 7**). Because we have estimated the content of condensed structures previously, we can determine the *β*-*O*-4′ content. The MWL was determined to contain 0.64 C/Ar, and because there are two carbons per moiety, there are 0.32 of these substructures per aromatic ring, coinciding precisely with the determination by solution NMR. A similar determination for REL indicates 0.78 C/Ar, or 0.39 substructures per aromatic ring (**Table 4**). It should be noted that the presence of other unknown structures can perturb this calculation as it is surprising that the REL would have a higher *β*-aryl ether content.

Carbohydrate Content. The C_1 carbon in pyranose ring based carbohydrate polymers (and free sugars) is the anomeric carbon. The C_1 can be separated by employing ^{13}C chemical shift anisotropy (CSA) combined with ^{13}C DP/MAS (*25*). As a result, the C_1 carbon and hence the carbohydrate content can be estimated by multiplying the content of C_1 by 6 or slightly less if five-membered sugar rings are taken into account. The REL was calculated from solid-state NMR to contain 15% carbohydrate, whereas MWL contains around 2%. Wet chemical analysis detected 14.4 and 0.5%, respectively, substantiating the effectiveness of the technique for estimating the carbohydrate content of intact lignocellulosics.

−-OCH3 Groups. The amounts of OCH_3 groups were obtained using DP/MAS with recoupled dipolar dephasing. A dipolar-dephasing factor 0.65 for OCH_3 is used to correct for the dephasing. On this basis, MWL and REL were calculated to be 1.12 and 1.15 OCH_3 per aromatic ring, respectively, consistent with the fact that this lignin is primarily G (**Table 3**).

Lignin Aliphatic Side-Chain Carbons. The spectrum from 98 to 61.2 ppm represents primarily lignin aliphatic side-chain structures and C_{2-6} from carbohydrates. The estimation of the content of the interunit linkages in lignin is challenging due to significant overlapping of their signals with those of carbohydrates. With our advanced NMR, we can more accurately estimate the contents of interunit linkages of lignin by subtracting the contribution of the carbohydrates between 98 and 61.2 ppm as determined from the C_1 integration (see above) based on DP/MAS with recoupled dipolar dephasing. **Table 4** shows that the calculation returns values of 2.95 and 2.97 C/Ar for the MWL and REL, respectively, which is close to the theoretical value of 3 per aromatic ring. It should be noted that all of the carbon integrations in **Tables 3** and **4** are balanced and are mathematically sensible estimations.

Aliphatic C—C Structures. The aliphatic C—C resonances in lignin are known to arise from condensed structures such as *β*-5′, *β*-*β*′, and *β*-1′ moieties, which are centered from 60 to 48 ppm and are overlapped in the solid-state DP/MAS spectrum. Although not quantitative, the C—H selection spectrum can supply an unimpeded aliphatic C—C integration, which can be compared to the aromatic C—H, returning values of 0.34 and 0.32 C/Ar for MWL and REL, respectively (**Table 4**). The MWL estimation is higher compared to solution NMR (0.14 C/Ar); however, it can be visually observed that the DP experiment exhibits more carbon

resonances in general for both MWL and REL in the upfield regions of the spectrum (61.2−0 ppm) compared with solution NMR. Although not absent from the solution NMR spectrum, these resonances are accentuated in the quantitative DP spectrum. If these are true structural components, they have not been observed previously in lignin preparations and indicate that there are as yet undetermined structural components.

Additional unknown methine carbons in the region from 48 to 30 ppm that are of unknown origin represent an additional 0.23 and 0.26 C/Ar for MWL and REL. The total integration from DP for MWL and REL are 0.38 and 0.28, respectively; therefore, by difference the two preparations contain 0.15 and 0.02 methylene C/Ar, respectively. Solution NMR returns a value of about 0.09 C/Ar for this region for MWL and is representative of minor structures such as dihydroconiferyl alcohol, secoisolariciresinol, **XIII**, and methylene carbons (**Table 4**).

Methyl Groups. The methyl content as determined by DP/MAS is much higher for both preparations than classically supposed by wood chemistry. It is typical that methyl groups in wood are attributed to acetyl groups in xylan (∼22 ppm). As expected, the REL indicates the presence of xylan-associated methyl groups, whereas the MWL does not. The methyl signals in the MWL spectrum (**Figure 3b**) and to a lesser extent the REL are largely dispersed across 24−10 ppm, indicating more diversity in structure than simply those derived from hemicellulose. Furthermore, the presence of a large resonance in this region of the spectrum is contrary to previous reports (*29*). Through direct polarization, the DP/MAS experiment produces contributions of 0.28 C/Ar for both preparations (**Table 4**).

Total Carbons. **Table 3** lists the breakdown of the total carbons integrated from the DP spectrum. The MWL contains 10.48 carbons per aromatic ring (C/Ar), which coincides with the theoretical calculation of 10 C derived directly from lignin with low residual carbohydrates. The REL spectrum contains 12.48 C/Ar, which is higher than theoretical but reflects the contributions from residual carbohydrates. As discussed above, the overall yield of carbons from different spectra balances quite well, indicating that the techniques proffered are very close to quantitative.

In summary, detailed structural information concerning the makeup of two lignin fractions, MWL and REL, is compared on the basis of quantitative DP/MAS, DP/MAS with recoupled dipolar decoupling, a range of spectral-editing techniques, and 2D HETCOR with ^{1}H spin diffusion. Our quantitative structural information, obtained using DP combined with spectral-editing techniques, indicates that REL contains much more residual carbohydrates than MWL. REL is also of higher −COO, aromatic C—C, and a much higher degree of condensed aromatic structure but of decreased aromatic C—H compared with MWL. In addition, REL and MWL contain similar amounts of ketones and aldehydes, OCH_3, aromatic C—O, lignin aliphatic side-chain carbons, and aliphatic C—C groups. At the spin diffusion time of 0.55 ms, the magnetization is equilibrated through the whole structure of MWL lignin, whereas the spin diffusion time required to equilibrate the magnetization throughout the whole structure of REL is 5.25 ms, indicating that REL is more heterogeneous than MWL, primarily due to more carbohydrate residues in REL. The present study provides more detailed lignin structural analysis than has been achieved previously using solid-state NMR.

ABBREVIATIONS USED

MWL, milled wood lignin; REL, residual enzyme lignin; CSA, ^{13}C chemical shift anisotropy filter; 2D HETCOR, two-dimensional ^{1}H−^{13}C heteronuclear correlation nuclear magnetic resonance; DP/MAS, direct polarization/magic angle spinning; DHP, dehydrogenation polymer; CEL, cellulolytic enzyme lignin; NMR, nuclear magnetic resonance; CP/T_1-TOSS, cross-polarization/spin−lattice relaxation time/total sideband suppression; CP/TOSS, cross-polarization/total sideband suppression; CP, cross-polarization; TOSS, total suppression of sidebands; TPPM, two-pulse phase-modulated; CP/MAS, cross-polarization/magic angle spinning; LGCP, Lee−Goldburg cross-polarization; HHCP, Hartmann−Hahn cross-polarization; DP, direct polarization; DD, dipolar dephasing; CH, C—H selection; diff, calculated by difference; H, *p*-hydroxyphenyl; G, guaiacyl; S, syringyl.

ACKNOWLEDGMENT

We are especially grateful to Prof. Klaus Schmidt-Rohr for his kind support.

LITERATURE CITED

(1) Higuchi, T. *Biosynthesis of Lignin*; Academic Press: New York, 1985; pp 141−160.
(2) Sarkanen, K. V. Precursors and their polymerization. In *Lignins: Occurrence, Formation, Structure and Reactions*; Sarkanen, K. V., Ludwig, C. H., Eds.; Wiley-Interscience: New York, 1971; pp 95−163.
(3) Sederoff, R. R.; Chang, H. M. Lignin biosynthesis. In *Wood Structure and Composition*; Lewin, M., Goldstein, I. S., Eds.; Dekker: New York, 1991; pp 263−286.
(4) Terashima, N.; Fukushima, K. Biogenesis and structure of macromolecular lignin in the cell wall of tree xylem as studied by microautoradiography. In *Plant Cell Wall Polymers, Biogenesis and Biodegradation*; Lewis, N. G., Paice, M. G., Eds.; American Chemical Society: Washington, DC, 1989; Vol. 399, pp 160−181.
(5) Goodwin, T. W.; Mercer, E. I. In *Introduction to Plant Biochemistry*; Pergamon Press: Oxford, U.K., 1972.
(6) Bjorkman, A. Isolation of lignin from finely divided wood with neutral solvents. *Nature* **1954**, *174*, 1057–1058.
(7) Bjorkman, A. Studies on finely divided wood. Part I. Extraction of lignin with neutral solvents. *Svensk Papperstidn*. **1956**, *59*, 477–485.
(8) Bjorkman, A. Studies on finely divided wood. Part 5. The effect of milling. *Svensk Papperstidn*. **1957**, *60*, 329–335.
(9) Bjorkman, A. Studies on finely divided wood. Part 3. Extraction of lignin−carbohydrate complexes with neutral solvents. *Svensk Papperstidn*. **1957**, *60*, 243–251.
(10) Bjorkman, A. Lignin and lignin-carbohydrate complexes. Extraction from wood meal with neutral solvents. *J. Ind. Eng. Chem*. **1957**, *49*, 1395–1398.
(11) Bjorkman, A.; Person, B. Studies on finely divided wood. Part 2. The properties of lignins extracted with neutral solvents from softwoods and hardwoods. *Svensk Papperstidn*. **1957**, *60*, 158–169.
(12) Chang, H. M.; Cowling, E. B.; Brown, W.; Adler, E.; Miksche, G. Comparative studies on cellulolytic enzyme lignin and milled wood lignin of sweetgum and spruce. *Holzforschung* **1975**, *29*, 153–159.
(13) Holtman, K. M.; Kadla, J. F. A solution-state NMR study of the similarities between MWL and CEL. *J. Agric. Food. Chem*. **2004**, *52*, 720–726.
(14) Holtman, K. M.; Chang, H.-M.; Kadla, J. F. An NMR comparison of the whole lignin from milled wood, MWL, and REL dissolved by the DMSO/NMI procedure. *J. Wood Chem. Technol*. **2007**, *27*, 179–200.
(15) Hu, Z. J.; Yeh, T. F.; Chang, H. M.; Matsumoto, Y.; Kadla, J. F. Elucidation of the structure of cellulolytic enzyme lignin. *Holzforschung* **2006**, *60*, 389–397.
(16) Ikeda, T.; Holtman, K.; Kadla, J. F.; Chang, H. M.; Jameel, H. Studies on the effect of ball milling on lignin structure using a modified DFRC method. *J. Agric. Food Chem*. **2002**, *50*, 129–135.
(17) Mao, J.-D.; Holtman, K. M.; Scott, J. T.; Kadla, J. F.; Schmidt-Rohr, K. Differences between lignin in unprocessed wood, milled wood, mutant wood, and extracted lignin detected by ^{13}C solid-state NMR. *J. Agric. Food Chem*. **2006**, *54*, 9677–9686.
(18) Mao, J.-D.; Cory, R. M.; McKnight, D. M.; Schmidt-Rohr, K. Characterization of a nitrogen-rich fulvic acid and its precursor algae from solid state NMR. *Org. Geochem*. **2007**, *38*, 1277–1292.

(19) Mao, J.-D.; Fang, X.; Schmidt-Rohr, K.; Carmo, A. M.; Hundal, L. S.; Thompson, M. L. Molecular-scale heterogeneity of humic acid in particle-size fractions of two Iowa soils. *Geoderma* **2007**, *140*, 17–29.

(20) Mao, J.-D.; Tremblay, L.; Gagné, J. P.; Kohl, S.; Rice, J.; Schmidt-Rohr, K. Humic acids from particulate organic matter in the Saguenay Fjord and the St. Lawrence Estuary investigated by advanced solid-state NMR. *Geochim. Cosmochim. Acta* **2007**, *71*, 5483–5499.

(21) Mao, J.-D.; Hu, W. G.; Schmidt-Rohr, K.; Davies, G.; Ghabbour, E. A.; Xing, B. S. Quantitative characterization of humic substances by solid-state carbon-13 nuclear magnetic resonance. *Soil Sci. Soc. Am. J.* **2000**, *64*, 873–884.

(22) Mao, J.-D.; Schmidt-Rohr, K. Accurate quantification of aromaticity and nonprotonated aromatic carbon fraction in natural organic matter by ^{13}C solid-state nuclear magnetic resonance. *Environ. Sci. Technol.* **2004**, *38*, 2680–2684.

(23) Dixon, W. T. Spinning-sideband-free and spinning-sideband-only NMR spectra in spinning samples. *J. Chem. Phys.* **1982**, *77*, 1800–1809.

(24) Mao, J.-D.; Schmidt-Rohr, K. Separation of aromatic-carbon ^{13}C NMR signals from di-oxygenated alkyl bands by a chemical-shift-anisotropy filter. *Solid State Nucl. Magn. Reson.* **2004**, *26*, 36–45.

(25) Schmidt-Rohr, K.; Mao, J. D. Efficient CH-group selection and identification in ^{13}C solid-state NMR by dipolar DEPT and ^{1}H chemical-shift filtering. *J. Am. Chem. Soc.* **2002**, *124*, 13938–13948.

(26) Mao, J.-D.; Hundal, L. S.; Schmidt-Rohr, K.; Thompson, M. L. Nuclear magnetic resonance and diffuse-reflectance Infrared Fourier transform spectroscopy of biosolids-derived biocolloidal organic matter. *Environ. Sci. Technol.* **2003**, *37*, 1751–1757.

(27) Martínez, A. T.; Almendros, G.; González-Vila, F. J.; Fründ, R. Solid-state spectroscopic analysis of lignins from several Austral hardwoods. *Solid State Nucl. Magn. Reson.* **1999**, *15*, 41–48.

(28) Mao, J.-D.; Hu, W.; Ding, G.; Schmidt-Rohr, K.; Davies, G.; Ghabbour, E.; Xing, B. Suitability of different ^{13}C solid-state NMR techniques in the characterization of humic acids. *Int. J. Environ. Anal. Chem.* **2002**, *82*, 183–196.

(29) Holtman, K. M.; Jameel, H.; Chang, H.; Kadla, J. F. Quantitative ^{13}C NMR characterization of milled wood lignins isolated by different milling techniques. *J. Wood Chem. Technol.* **2006**, *26*, 21–34.

(30) Chen, C.-L.; Robert, D. Characterization of lignin by ^{1}H and ^{13}C NMR spectroscopy. In *Methods in Enzymology*; Wood, W. A., Kellogg, S. T., Eds.; Academic Press: San Diego, CA, 1988; Vol. 137−174, p 2v.

(31) Chen, C.-L.; Robert, D. Characterization of milled wood lignins and dehydrogenative polymerisates from monolignols by carbon-13 NMR spectroscopy. In *Lignin and Lignan Biosynthesis*; Lewis, N., Sarkanen, S., Eds.; ACS Symposium Series 697; American Chemical Society: Washington, DC, 1998; pp 255−275.

(32) Capanema, E. A.; Balakshin, M. Y.; Kadla, J. F. A comprehensive approach for quantitative lignin characterization by NMR spectroscopy. *J. Agric. Food Chem.* **2004**, *52*, 1850–1860.

Received for review April 5, 2010. Revised manuscript received August 3, 2010. Accepted August 5, 2010. We thank the National Science Foundation (EAR- 0843996 and CBET-0853950) for financial support.